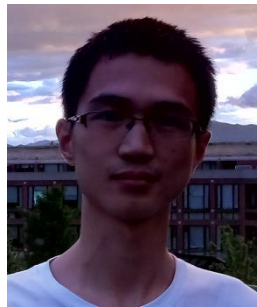


Orbital magnetization,
geometric phase,
and a modern theory of magnetic breakdown



A. Alexandradinata
Yale



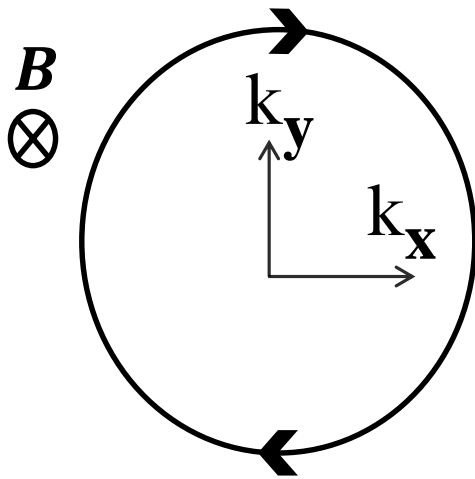
Wang Chong
Tsinghua



Leonid Glazman
Yale

Semiclassical theory of Bloch electrons in a magnetic field

A method to calculate wavefunctions and energy levels which become increasingly accurate in the limit that a **classical action function (A)** becomes much larger than a parameter characteristic of the field.



example: closed orbit

Hamilton's equation $\dot{\mathbf{k}} = \frac{e}{c} \nabla_{\mathbf{k}} \varepsilon \times \mathbf{B}$

Semiclassics hold when

the area of orbit $A \gg l^{-2} = eB/\hbar c$

inverse square of magnetic length

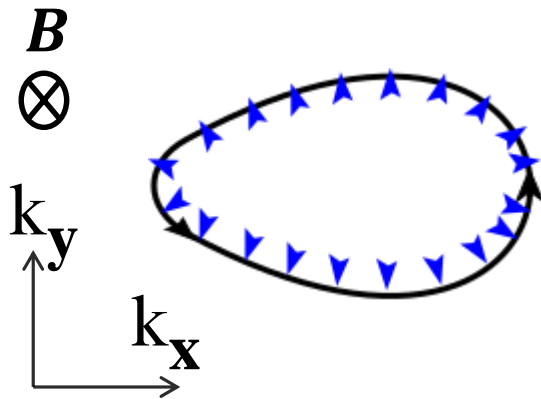
Modern notions in the semiclassical theory

developed in wavepacket and effective-Hamiltonian theory

(Chang, Sundaram et al, Qian Niu, Culcer et al)

(Roth,Blount,Kohn)

Geometric phase



$$\text{Berry phase} \quad \exp \left(i \oint \boldsymbol{\mathcal{X}} \cdot d\mathbf{k} \right)$$

$$\boldsymbol{\mathcal{X}}(\mathbf{k})_{mn} = i \langle u_{m\mathbf{k}} | \nabla_{\mathbf{k}} u_{n\mathbf{k}} \rangle$$

periodic component
of a Bloch function

For a pseudospin-half $H(\mathbf{k}) = \mathbf{R}(\mathbf{k}) \cdot \boldsymbol{\sigma}$,
the Berry phase is half the solid angle
subtended by the three-vector $\mathbf{R}(\mathbf{k})$.

If a symmetry enforces $\mathbf{R}(\mathbf{k})$ to lie in a plane,
the solid angle is 2π .

Modern notions in the semiclassical theory II

Orbital magnetic moment in atoms

Correction to groundstate energy

$$\Delta E = \mu_B \mathbf{B} \cdot \langle 0 | \mathbf{L} | 0 \rangle$$

$$\mathbf{L} = \sum_i \mathbf{r}_i \times \mathbf{p}_i$$

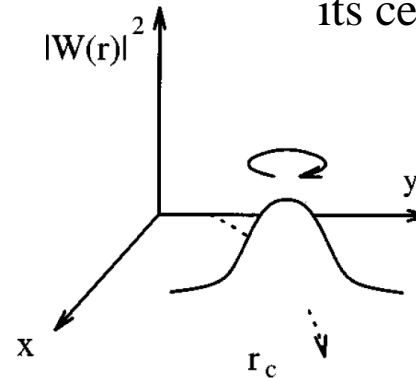
If $|0\rangle$ is nondegenerate, then time-reversal symmetry enforces $\Delta E = 0$.

T-invariant **solids** can have nonzero orbital magnetization owing to its action on the **crystal** momentum

$$T: \mathbf{k} \rightarrow -\mathbf{k}$$

Orbital magnetic moment in solids

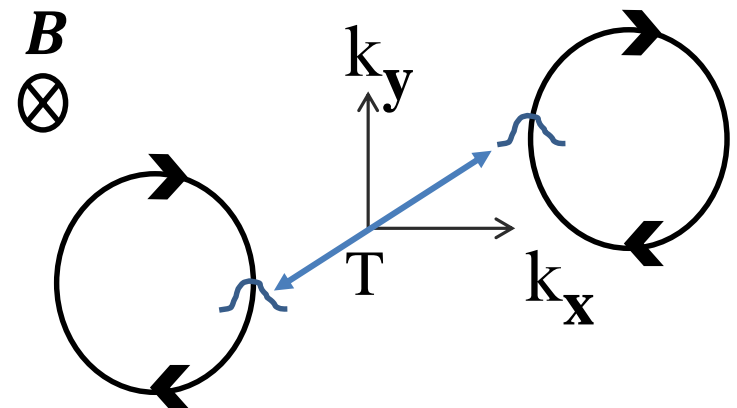
orbital angular momentum of a wavepacket rotating about its center of mass



(Chang, Niu, PRB 53, 7010)

Correction to energy of wavepacket $|w\rangle$

$$\Delta E = \mu_B \mathbf{B} \cdot \langle w | (\mathbf{r} - \mathbf{r}_c) \times \mathbf{p} | w \rangle$$



These modern notions refine the Bohr-Sommerfeld quantization conditions.

Review of traditional Bohr-Sommerfeld

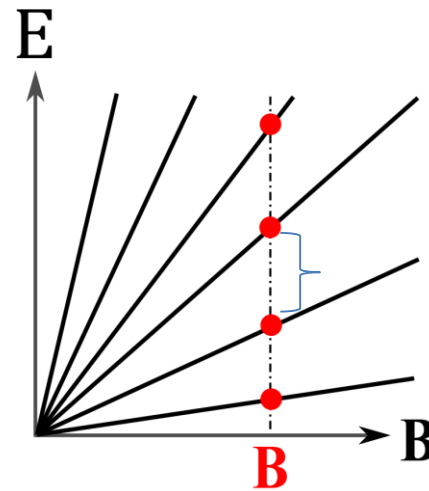
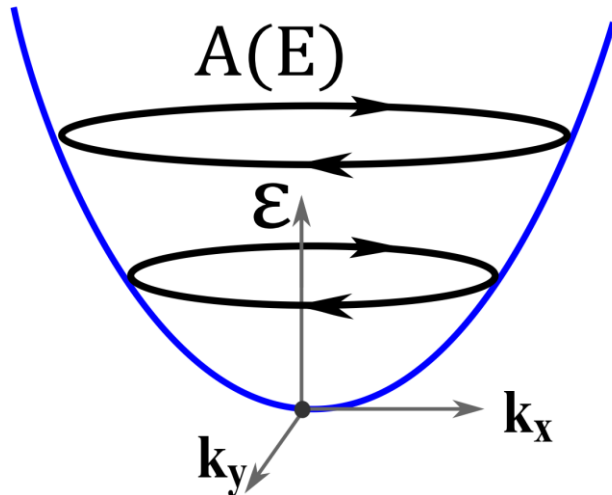
Onsager-Lifshitz: $l^2 A(E_n) = \pi(2n + 1) \quad n \in \mathbb{Z} \quad l^{-2} = eB/\hbar c$

For fixed field \mathbf{B} ,
discrete energetic solutions are Landau levels.

Maslov correction 'Zero-point energy
from quantum fluctuations'

Ex. Schrodinger $\varepsilon = (k_x^2 + k_y^2)/2m$

$$A(E) = \pi(k_x^2 + k_y^2) = 2\pi m E$$



$$\frac{2\pi}{l^2 m} = \frac{2\pi}{l^2 (dA/dE)}$$

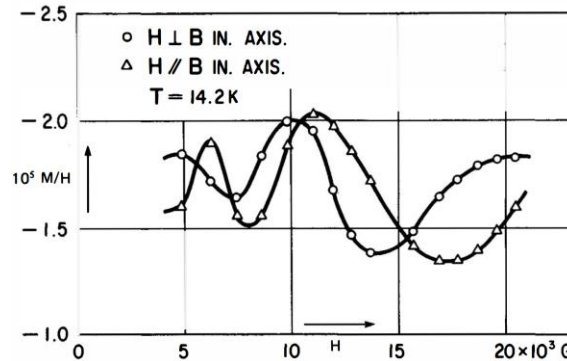
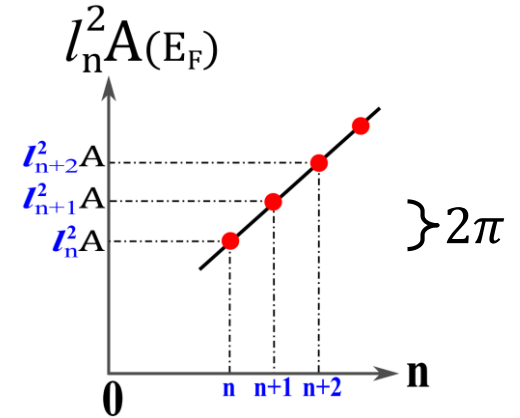
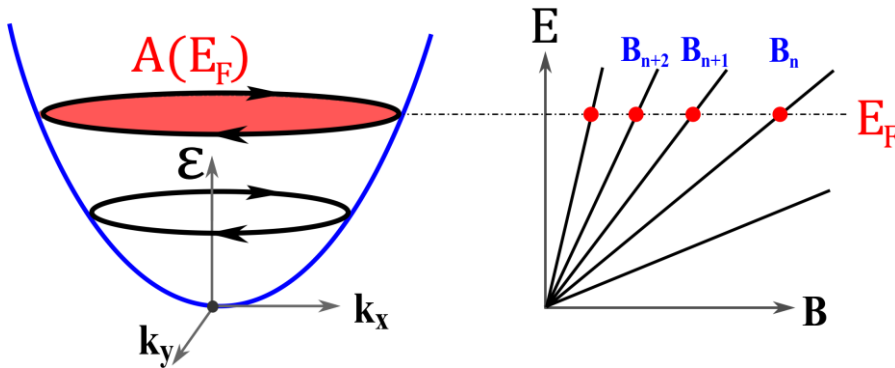
Effective mass
= dA/dE

At fixed Fermi energy, l_n^2 are values of the inverse fields where Landau levels successively become equal to the Fermi energy.

$$l_n^2 A(E_F) = \pi(2n + 1)$$

$$l_{n+1}^2 - l_n^2 = 2\pi / A(E_F)$$

leads to dHvA oscillations.



First observation in Bismuth de Haas, van Alphen (1930)

Phenomenology of relating magnetic phenomenon the **shape** of the Fermi surface:
‘Fermiology’ of metals

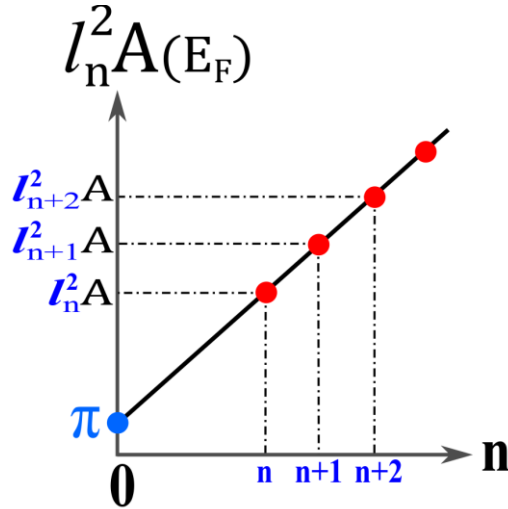
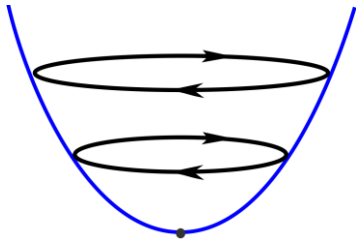
Relate magnetic phenomenon to **robust** properties of the Fermi-surface **wavefunction**:
‘**Topo-Fermiology**’

Infinite-field intercept of dHvA oscillations

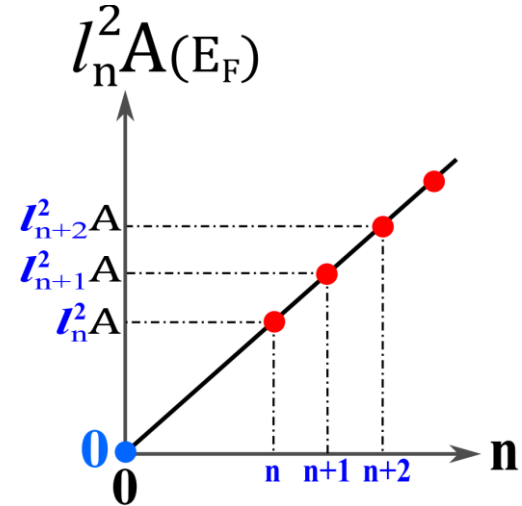
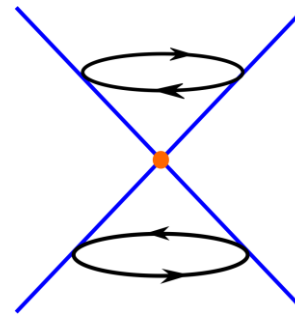
Onsager-Lifshitz: $l_0^2 A(E_F) =$

π **γ -intercept**
Maslov

Ex. 1: Schrodinger



Ex. 2: Dirac



To find a Dirac point
without ever seeing it.

Standard lore for **nondegenerate** band

$$\gamma\text{-intercept} = \pi + \begin{cases} 0, & \text{Schrodinger} \\ \pi, & \text{Dirac} \end{cases}$$

(Berry, Mikitik PRL 82 2147)

For D-fold degenerate bands, (e.g., D=2: spin-degeneracy)

$$l^2 A(E) = 2\pi n + \underbrace{\pi - \lambda_\alpha}_{\text{intercept}} \quad \text{Beyond Onsager} \quad \alpha = 1, \dots, D$$

$\{\lambda_\alpha\}$ encodes the modern corrections

- (i) orbital magnetization (vanishes in centrosymmetric metals without SOC)
- (ii) the geometric phase (*non-abelian* for D>1, and generally a *continuous* quantity).

At fixed l^2 , solutions ($E_{n,\alpha}$) correspond to D sets of sub-Landau levels.

At fixed E, solutions ($l_{n,\alpha}^2$) correspond to D sub-harmonics in the dHvA;

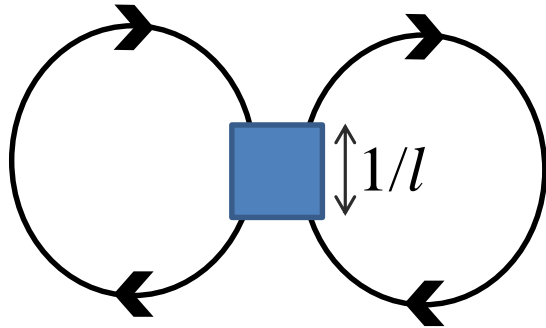
each sub-harmonic has its own intercept $\gamma_\alpha = \pi - \lambda_\alpha$.

Our contribution:

- (a) gauge-independent formulation of $\{\lambda_\alpha\}$ for multi-band quantization rule
(Gauge-dependent formulations for D=2 by Roth, Mikitik)
- (b) symmetry analysis determines in which solids, and for which field orientation,
 - is the Berry phase discrete/continuous?
 - is the orbital moment nonvanishing?
 - is γ_α/π rational and robust to Hamiltonian deformations?

γ_α/π are the topological invariants in magnetotransport

Beyond semiclassical theory



Magnetic breakdown

(Cohen,Falicov,Blount,Pippard,Azbel,Chambers,Slutskin)

The geometric phase and orbital moment are quantities defined on orbits.

Semiclassical orbits are no longer well-defined in the presence of quantum tunneling.

Can the modern semiclassical concepts be combined with quantum tunneling?

Modern theory of magnetic breakdown

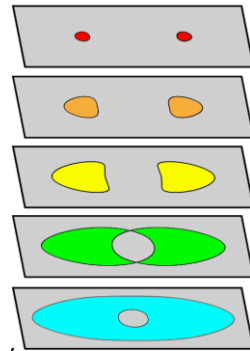
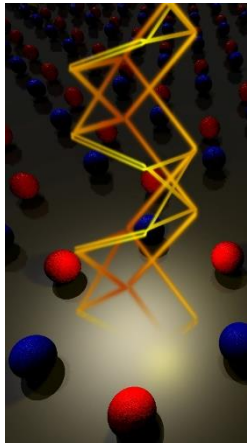
Our contribution:

Generalized Bohr-Sommerfeld quantization conditions that are beyond semiclassical, i.e., they incorporate GP,OM and MB.

Analytic, quantitative understanding of magnetic energy levels and dHvA peaks.

Many topological bandstructures, with unremovable geometric phase, unavoidably undergo breakdown.

Surface states of topological insulators



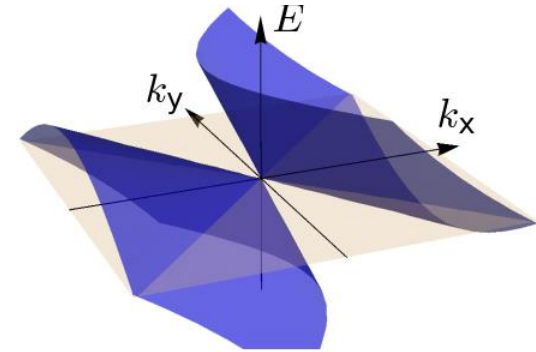
Hourglass fermions

(AA, Z.Wang,Bernevig
prx 6, 021008)

SnTe

(T. Hsieh, L. Fu,
Nat. Comm 3:982)

Topological metals



Tilted Dirac/Weyl fermion

(Soluyanov,Bernevig, Nature 527, 495;
Isobe, PRL 116, 116803;
Muechler, AA,Neupert,Car PRX 6, 041069)

Outline

Effective Hamiltonian of a Bloch electron in a magnetic field

Bohr-Sommerfeld quantization conditions for closed orbits.

Symmetry analysis of the quantization condition.

Formulate topological invariants in magnetic transport.

Quantization conditions that incorporate breakdown.

Effective Hamiltonian of a Bloch electron in a magnetic field

(Peierls,Luttinger,Wannier,Fredkin,Roth,Blount,Kohn,Zak,Nenciu)

Aim: describe dynamics within a low-energy subspace spanned by D degenerate bands.

Solution: identify a good quantum-mechanical representation, i.e., basis functions.

$$\phi_{n\mathbf{k}}(\mathbf{r}) = e^{i\mathbf{k}\cdot\mathbf{r}} u_{n,\mathbf{k}+\mathbf{a}(\mathbf{r})}(\mathbf{r})$$

Field-modified Bloch functions form a representation of magnetic translations

(Brown,Zak,Misra)

$$(\hat{H} - E)\Psi = 0 \quad \Psi(\mathbf{r}) = \sum_{n\mathbf{k}} g_{n\mathbf{k}} \phi_{n\mathbf{k}}(\mathbf{r})$$

$$\sum_{n=1}^D (\mathcal{H}(\mathbf{K})_{mn} - E \delta_{mn}) g_{n\mathbf{k}} = 0$$

$\mathcal{H}(\mathbf{K})$, the effective Hamiltonian, is a symmetrized function of the kinematic quasimomentum operator:

$$\mathbf{K} = \mathbf{k} + \mathbf{a}(i\nabla_{\mathbf{k}}) \quad \mathbf{K} \times \mathbf{K} = -i\frac{e}{c}\mathbf{B}$$

$$\mathcal{H}(\mathbf{K}) = H_0(\mathbf{K}) + H_1(\mathbf{K}) + H_2(\mathbf{K}) + \dots \quad H_j(\mathbf{k}) = O(B^j)$$

$$H_0(\mathbf{k}) = \varepsilon_{n\mathbf{k}} \quad \text{Peierls-Onsager Hamiltonian}$$

To leading order in B , dynamics occurs within the low-energy subspace.

To next order in B ,
interband transitions occur between low- and high-energy subspaces.

Beyond the Peierls-Onsager theory

(Roth,Blount,Kohn)

$$H_1(\mathbf{k}) = H_1^B + H_1^{OM} + H_1^Z$$

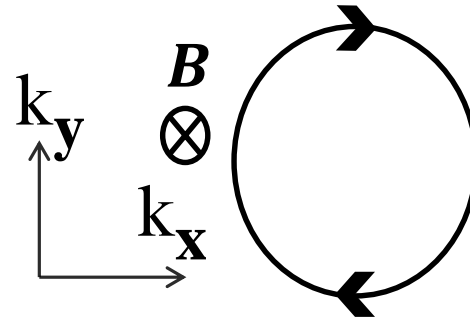
generates the **Berry** phase

$B \times$ **orbital moment**

Zeeman coupling

$$\exp\left(-i \oint H_1^B dt\right) = \exp\left(i \oint \mathfrak{X} \cdot d\mathbf{k}\right)$$

$$\mathfrak{X}(\mathbf{k})_{mn} = i \langle u_{m\mathbf{k}} | \nabla_{\mathbf{k}} u_{n\mathbf{k}} \rangle$$



$$H_1^{OM} = \mu_B \mathbf{B} \cdot \mathbf{r}_{\text{off}} \times \mathbf{p}_{\text{off}} \quad (\text{off-diagonal w.r.t. to low- and high-energy subspaces})$$

$$= \mu_B B \sum_{\bar{m} \neq n} i \langle u_{n\mathbf{k}} | \nabla_{\mathbf{k}}^x u_{\bar{m}\mathbf{k}} \rangle \langle u_{\bar{m}\mathbf{k}} | \hat{p}^y | u_{n\mathbf{k}} \rangle - (x \leftrightarrow y)$$

Terms analogous to H_1^B and H_1^{OM} appear ubiquitously
in the asymptotic theory of coupled wave equations

(Littlejohn,Flynn,PRA 44,5239)

The effective Hamiltonian does not depend on its basis in the usual way.

$$|u_{n\mathbf{k}}\rangle \rightarrow \sum_{m=1}^D |u_{m\mathbf{k}}\rangle V_{mn}(\mathbf{k}), \quad V^{-1} = V^\dagger$$

What we have shown:

For Chern insulators with short-ranged hoppings,

$$H_1 \not\rightarrow V^{-1}H_1V.$$

For symmetry-protected topological insulators,

H_1 transforms anomalously under symmetry.

The theory of effective Hamiltonians is fundamentally a gauge theory.

Basic gauge-covariant objects: ‘Wilson loops’

$$\mathcal{P} \exp \left(-i \int H_1 dt \right) \longrightarrow V^{-1} \mathcal{P} \exp \left(-i \int H_1 dt \right) V$$

Gauge-invariant eigenvalues $\{e^{i\lambda_\alpha}\}$ enter the quantization condition.

Wilson loops appear in the WKB wavefunction of effective Hamiltonians

$$(H_0(\mathbf{K}) + H_1(\mathbf{K}) - E)g(\mathbf{k}) = 0$$

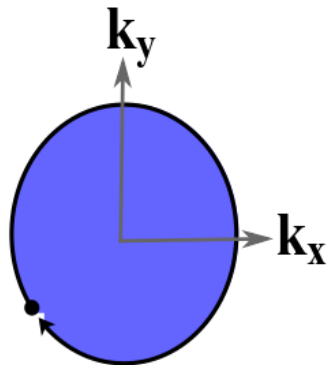
$$K_x = k_x + il^{-2}\partial_y, \quad K_y = k_y$$

vector wavefunction $\mathcal{P} \exp \left(-il^2 \int (k_x - H_1(\frac{\partial \varepsilon}{\partial k_x})^{-1}) dk_y \right) * g(\mathbf{0})$

k-independent vector.

Quantities in the exponent
are evaluated on the band contour.

(Generalizes single-band
wavefunction by
Zilberman, Fischbeck)



sweeps out the area (**A**)
of the circle

generates the propagator

$$\mathcal{P} \exp \left(-i \int H_1 dt \right)$$

with eigenvalues $\{e^{i\lambda_\alpha}\}$
 $\alpha = 1, \dots, D$

Quantization condition for closed orbits

is equivalent to imposing continuity of (vector) wavefunction around a loop

$$l^2 \mathbf{A} = 2\pi n - \lambda_\alpha + \pi$$

Maslov

$$l^2 A = 2\pi n - \lambda_a + \pi$$

dHvA intercepts $\gamma_a = -\lambda_a + \pi$ ($\pm\pi/4$ Lifshitz-Kosevich correction in 3D)

In some solids, and for certain field orientations,
 λ_a/π (and hence γ_a/π)
is symmetry-fixed to a rational number.

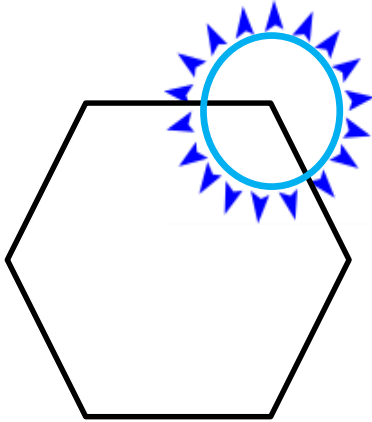
γ_a are the topological invariants of magnetotransport.

Case studies: graphene, Bi₂Se₃, 3D Weyl metals (WTe₂), SnTe, WSe₂

Role of symmetry and field orientation in rationalizing γ_a/π .

2D spinless Dirac point

(ex: Graphene)



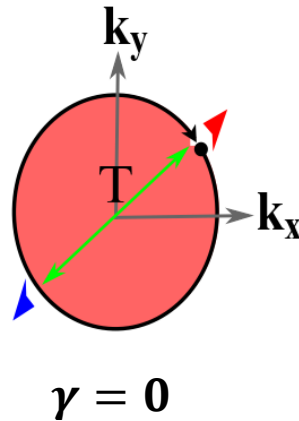
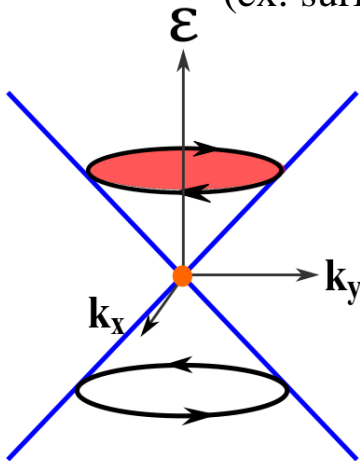
Spacetime-inversion symmetry:
like a time-reversal symmetry that maps $\mathbf{k} \rightarrow \mathbf{k}$

Sublattice pseudospin lies in plane:
Berry phase of π ,
Orbital magnetization is suppressed.

$$\gamma = 0$$

2D spinful Dirac point

(ex: surface of Bi₂Se₃)

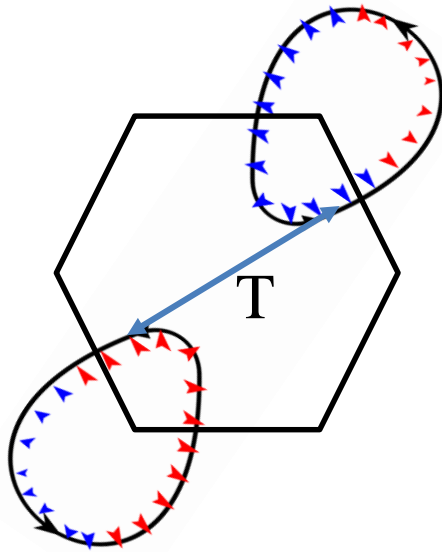


Due to T symmetry acting as $\mathbf{k} \rightarrow -\mathbf{k}$,
pseudospins cant in opposite directions.

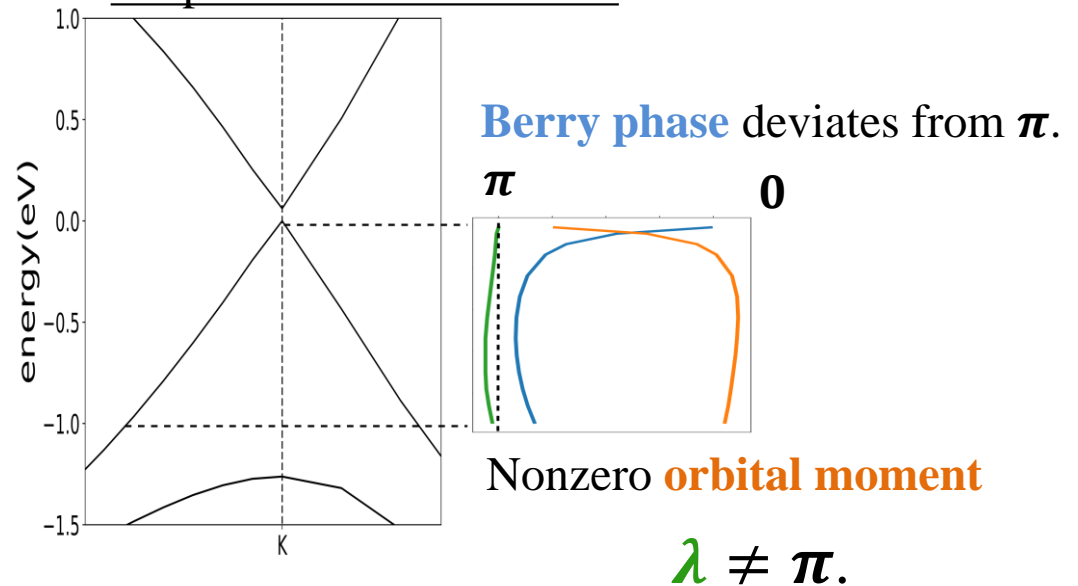
$$\gamma = 0$$

Time-reversal-related massive Dirac fermions

Spinless graphene with broken spatial-inversion symmetry:
no $\mathbf{k} \rightarrow \mathbf{k}$ constraint.



Graphene on BN substrate

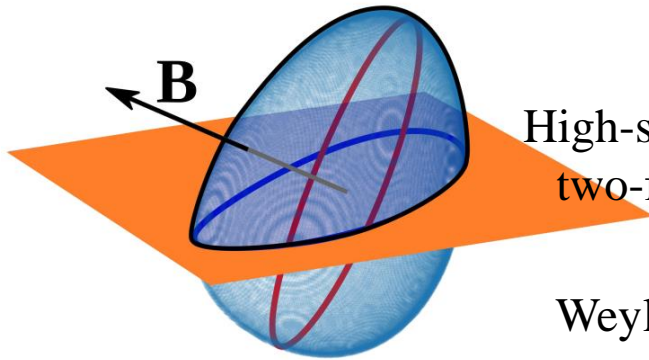


Due to T symmetry acting as $\mathbf{k} \rightarrow -\mathbf{k}$, pseudospins on different orbits cant in opposite directions.

Each valley-centered orbit produces a dHvA harmonic,
and the two intercepts are symmetry related: $\gamma_1 = -\gamma_2$.

2D solids: γ/π deviates from rationality when a spatial symmetry is broken.

3D solids: one can change the symmetry of the extremal orbit (and hence γ) by tilting the field with respect to a crystal axis.

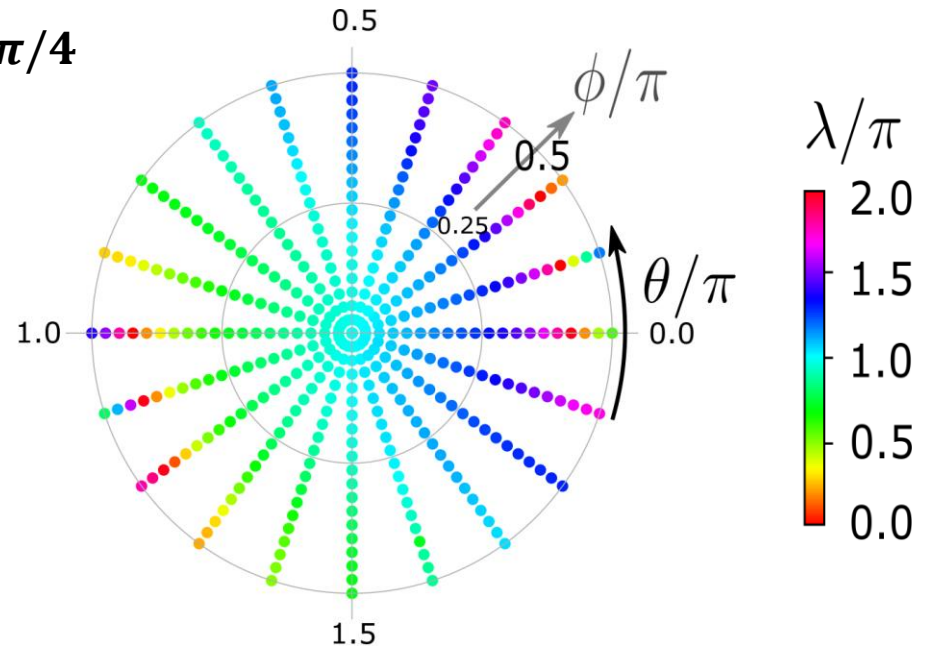
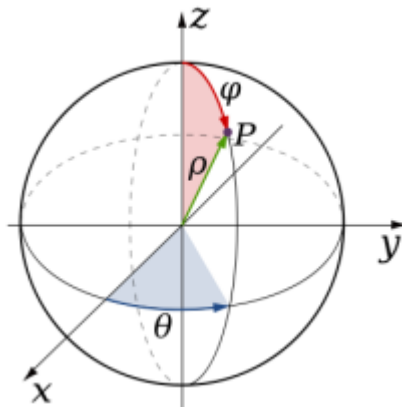


High-symmetry plane invariant under two-fold rotation and time reversal

Weyl fermion centered on a generic wavevector on the plane.
(e.g., strained WTe₂, Soluyanov et al)

Symmetric extremal orbit $\lambda = \pi$, $\gamma = -\pi/4$

Asymmetric extremal orbit $\gamma \neq -\pi/4$



For which solids and field orientations are

λ_a/π (and hence γ_a/π)
symmetry-fixed to rationality?

10 (and only 10) classes of closed, symmetric orbits.

Each class corresponds to a unique group algebra for the propagator

$$\mathcal{A} = \mathcal{P} \exp \left(-i \int H_1 dt \right)$$

Constraints on λ_a are derived from this algebra.

	u	s	Algebra	Representation
(I) $\forall \mathbf{k}^\perp,$	0	0	$\mathcal{A} = \bar{g} \mathcal{A} \bar{g}^{-1}$	$\bar{g}^2 = e^{i\pi F a - i\mathbf{k} \cdot \mathbf{R}}$
$\mathbf{k}^\perp = g \circ \mathbf{k}^\perp$	0	1	$\mathcal{A} = \bar{g} \mathcal{A}^* \bar{g}^{-1}$	$(\bar{g} K)^2 = e^{i\pi F a - i\mathbf{k} \cdot \mathbf{R}}$
(II-A)	0	0	$\mathcal{A} = \bar{g} \mathcal{A} \bar{g}^{-1}$	$\bar{g}^N = \mathcal{A}^{\pm N/L} e^{i\pi F a}$
$\mathbf{k}^\perp \in \mathfrak{o},$	0	1	$\mathcal{A} = \bar{g} \mathcal{A}^* \bar{g}^{-1}$	$(\bar{g} K)^N = \mathcal{A}^{\pm N/L} e^{i\pi F a}$
$ \mathfrak{o} = g \circ \mathfrak{o} $	1	0	$\mathcal{A} = \bar{g} \mathcal{A}^{-1} \bar{g}^{-1}$	$\bar{g}^N = e^{i\pi F a - i\mathbf{k} \cdot \mathbf{R}}$
	1	1	$\mathcal{A} = \bar{g} \mathcal{A}^t \bar{g}^{-1}$	$(\bar{g} K)^N = e^{i\pi F a - i\mathbf{k} \cdot \mathbf{R}}$
(II-B)	0	0	$\mathcal{A}_{i+1} = \bar{g}_i \mathcal{A}_i \bar{g}_i^{-1}$	$\bar{g}_N \dots \bar{g}_1 = e^{i\pi F a - i\mathbf{k} \cdot \mathbf{R}}$
$\mathbf{k}^\perp \in \mathfrak{o},$	0	1	$\mathcal{A}_{i+1} = \bar{g}_i \mathcal{A}_i^* \bar{g}_i^{-1}$	$\bar{g}_N K \dots \bar{g}_1 K = e^{i\pi F a - i\mathbf{k} \cdot \mathbf{R}}$
$ \mathfrak{o} \neq g \circ \mathfrak{o} $	1	0	$\mathcal{A}_{i+1} = \bar{g}_i \mathcal{A}_i^{-1} \bar{g}_i^{-1}$	$\bar{g}_N \dots \bar{g}_1 = e^{i\pi F a - i\mathbf{k} \cdot \mathbf{R}}$
	1	1	$\mathcal{A}_{i+1} = \bar{g}_i \mathcal{A}_i^t \bar{g}_i^{-1}$	$\bar{g}_N K \dots \bar{g}_1 K = e^{i\pi F a - i\mathbf{k} \cdot \mathbf{R}}$

Rational

Rational

Rational

Landau-level degeneracy

Symmetric splitting

Symmetric splitting

Landau-level degeneracy

Why only 10 classes of symmetric orbits?

For any symmetry g , three distinct types of mappings in 2D \mathbf{k} -space:

Class I: $\mathbf{k} \rightarrow \mathbf{k}$

Class II: $\mathbf{k} \rightarrow g \circ \mathbf{k} \neq \mathbf{k}$

Class II-A: \mathbf{k} and $g \circ \mathbf{k}$ lie on the same orbit

Class II-B: \mathbf{k} and $g \circ \mathbf{k}$ on distinct orbits

$u=0$ (orientation-preserving), 1 (reflection)

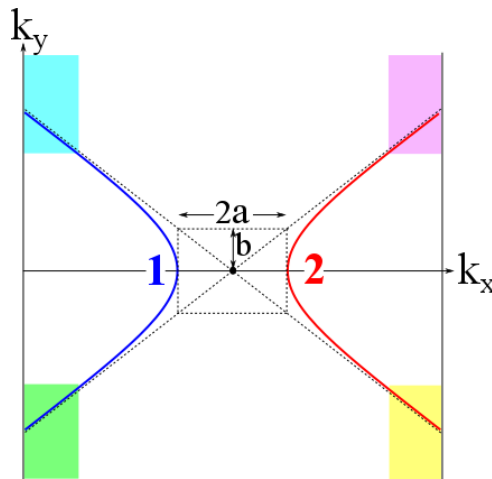
$s=1$ (includes time reversal), 0 (purely spatial transformation)

(I) $\forall \mathbf{k}^\perp,$ $\mathbf{k}^\perp = g \circ \mathbf{k}^\perp$	Graphene	λ	
		—	
		$e^{i\sum_a \lambda_a} \in \mathbb{R}$	Rational
(II-A)	Surface of Bi ₂ Se ₃	—	
$\mathbf{k}^\perp \in \mathfrak{o},$	Surface of SnTe	$e^{i\sum_a \lambda_a} \in \mathbb{R}$	Rational
$ \mathfrak{o} = g \circ \mathfrak{o} $		$e^{i\sum_a \lambda_a} \in \mathbb{R}$	Rational
		—	
(II-B)	Bilayer graphene	$\{\lambda_a^{i+1}\} = \{\lambda_a^i\}$	Landau-level degeneracy
$\mathbf{k}^\perp \in \mathfrak{o},$	Deformed graphene, WSe ₂	$\{\lambda_a^{i+1}\} = \{-\lambda_a^i\}$	Symmetric splitting
$ \mathfrak{o} \neq g \circ \mathfrak{o} $		$\{\lambda_a^{i+1}\} = \{-\lambda_a^i\}$	Symmetric splitting
		$\{\lambda_a^{i+1}\} = \{\lambda_a^i\}$	Landau-level degeneracy

Magnetic breakdown

(Cohen,Falicov,Blount,Pippard,Azbel,Chambers,Slutskin)

Within the breakdown region, band contours approach each other hyperbolically.



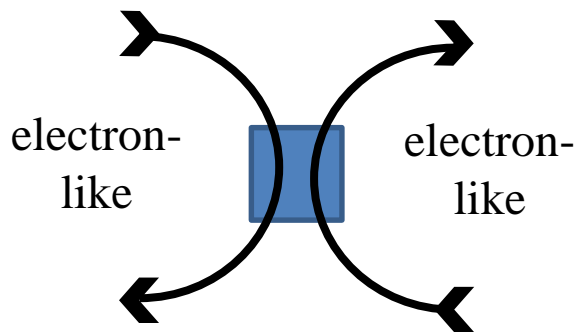
Dimensionless parameter
in breakdown region

$$\mu \propto abl^2$$

Breakdown is insignificant if

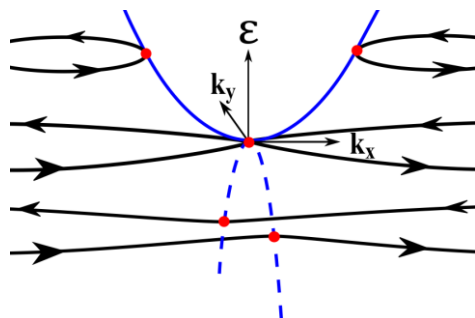
$$|\mu| \gg 1$$

The orientation of travelling wavepackets distinguish two qualitatively distinct types of breakdown.

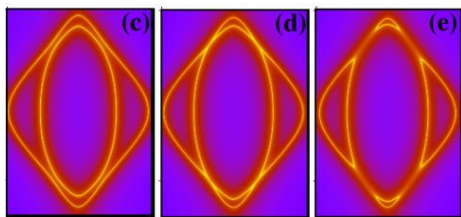


Two contours belong to the same band.

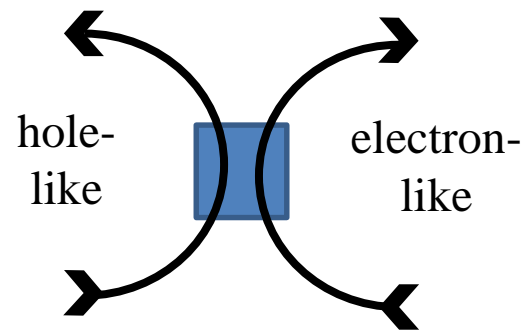
Intraband breakdown



The saddlepoint is the nucleus of Lifshitz transitions.

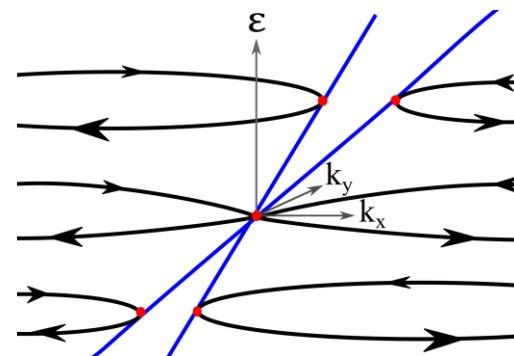


Hourglass fermion
KHgSb



The two contours belong to different bands.

Interband breakdown



Line nodes in 3D metals.
Over-tilted Weyl/Dirac points.

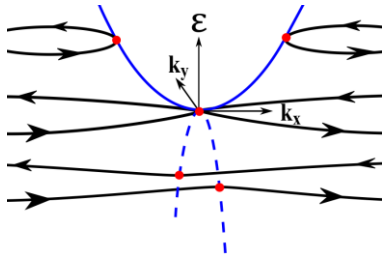
Goals

Magnetic energy levels and dHvA peaks are determined by generalized Bohr-Sommerfeld quantization rules that unify tunneling, geometric phase and the orbital moment.

Formulate topological invariant that:

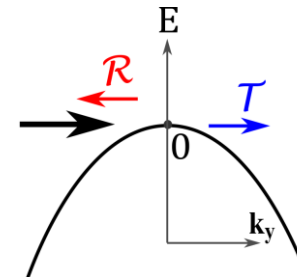
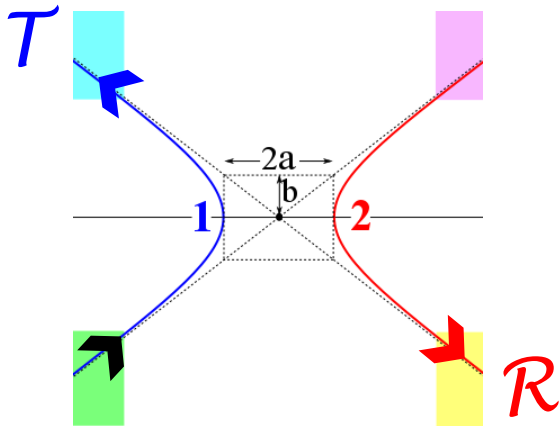
- (i) non-perturbatively encodes quantum tunneling,
- (ii) distinguishes metals with differing Berry phases on their Fermi surface.

Intraband breakdown



$$\varepsilon_{\mathbf{k}} = \frac{k_x^2}{2m_1} - \frac{k_y^2}{2m_2} \quad \longrightarrow \quad \frac{1}{2m_1} \left(k_x + i l^{-2} \frac{\partial}{\partial k_y} \right)^2 - \frac{k_y^2}{2m_2}$$

A Schrodinger particle with $\hbar = l^{-2}$, coordinate = k_y .



At zero energy ($\mu = 0$),

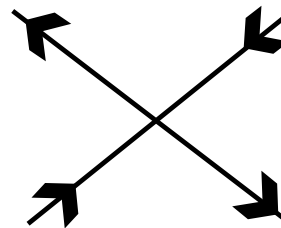
$$|\mathcal{R}|^2 = |\mathcal{T}|^2 = 1/2 \quad (\text{Kemle})$$

Semiclassics ‘breaks down’

Dimensionless parameter

$$\begin{aligned} \mu &= \sqrt{m_1 m_2} l^2 E \\ &= \frac{1}{2} a b l^2 \text{sign}[E] \end{aligned}$$

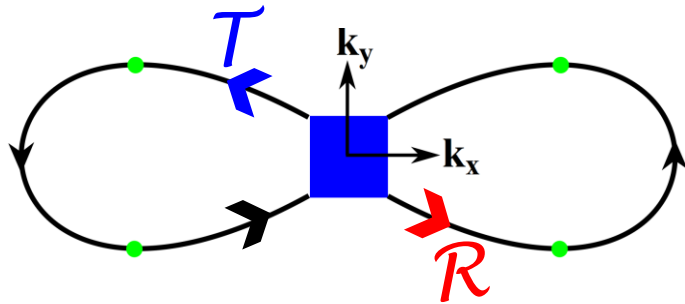
with E measured from the saddlepoint.



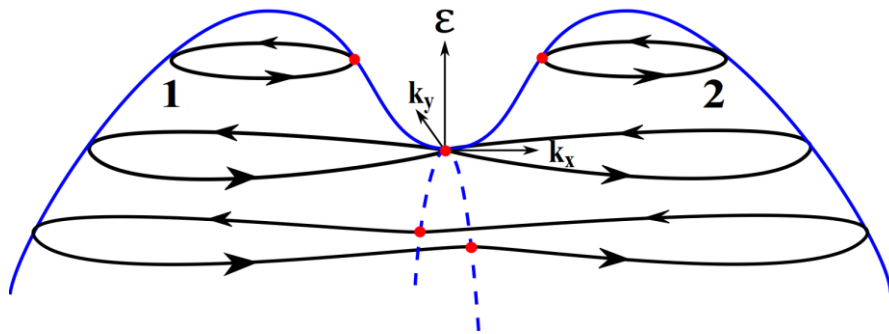
$$\dot{\mathbf{k}} = \frac{e}{c} \nabla_{\mathbf{k}} \varepsilon \times \mathbf{B} \rightarrow \mathbf{0}$$

A hypothetical wavepacket never reaches the saddlepoint in finite time.

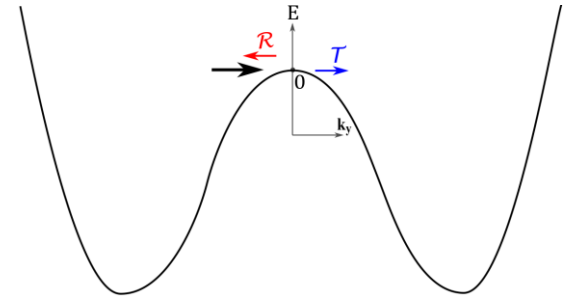
Two orbits merge into one.



Conventional metal

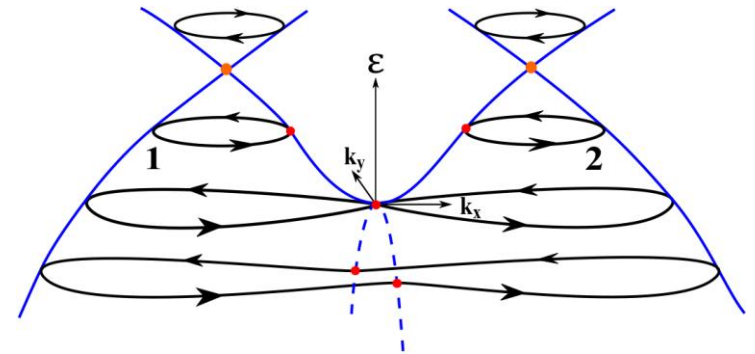


Analogy: double well



Topological metal

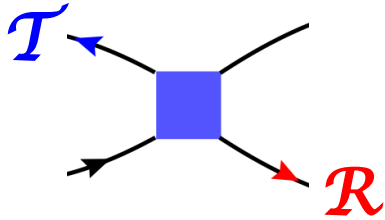
near a metal-insulator phase transition



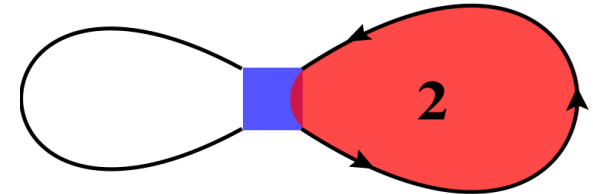
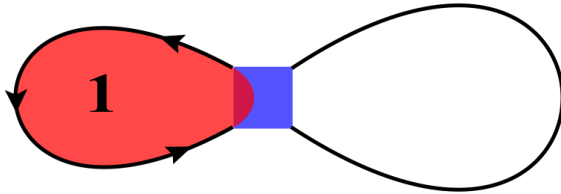
ex: strained graphene

Quantization condition

$$\cos\left(\frac{\Omega_1 + \Omega_2}{2} + \text{phase}(\mathcal{T})\right) = |\mathcal{T}| \cos\left(\frac{\Omega_1 - \Omega_2}{2}\right)$$



$$\mathcal{T} = \frac{e^{\pi\mu/2}}{\sqrt{2 \cosh(\pi\mu)}} e^{i \arg[\Gamma(1/2 - i\mu)] + \mu \log |\mu| - \mu}$$



Ω_1 = semiclassical phase acquired by wavepacket around a closed Feynman trajectory.

$$\Omega_j = -l^2 A_j(E) + \pi + \varphi_B$$

$$\varphi_B = \begin{cases} 0, & \text{(conventional)} \\ \pi, & \text{(topological)} \end{cases}$$

Continuity of wavefunction of the effective Hamiltonian:

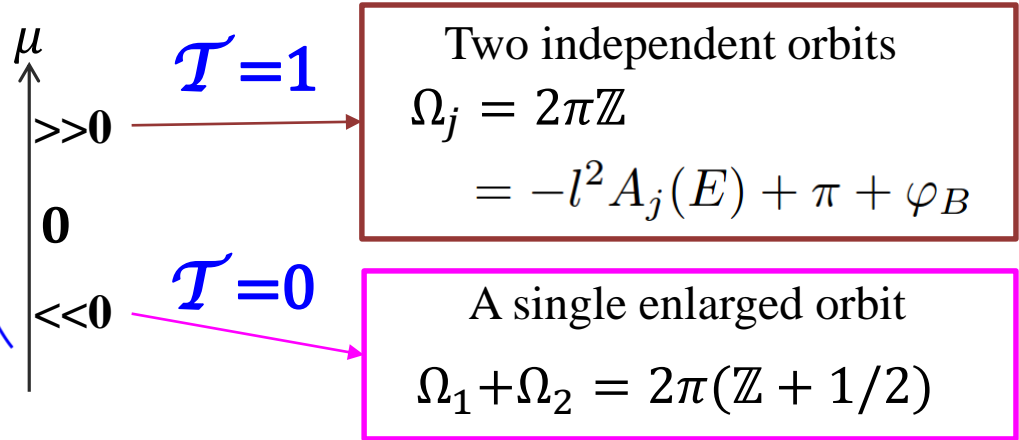
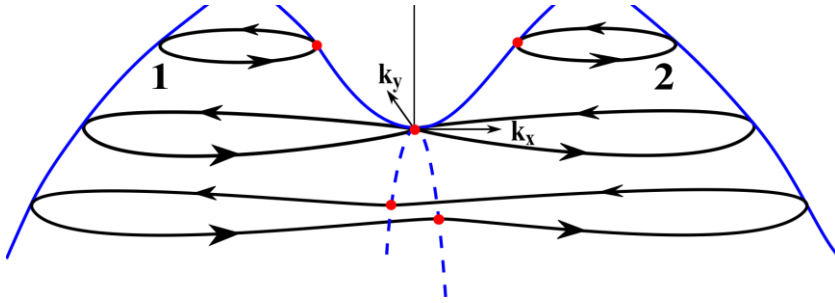
$$\det \left[\begin{pmatrix} \mathcal{T} & \mathcal{R} \\ \mathcal{R} & \mathcal{T} \end{pmatrix} \begin{pmatrix} e^{i\Omega_1} & 0 \\ 0 & e^{i\Omega_2} \end{pmatrix} - I \right] = 0$$

Scattering matrix

Semiclasical evolution

Quantization condition

$$\cos\left(\frac{\Omega_1 + \Omega_2}{2} + \text{phase}(\mathcal{T})\right) = |\mathcal{T}| \cos\left(\frac{\Omega_1 - \Omega_2}{2}\right)$$



$\mathcal{T} = 1$

Two independent orbits

$$\Omega_j = 2\pi\mathbb{Z}$$

$$= -l^2 A_j(E) + \pi + \varphi_B$$

$\mathcal{T} = 0$

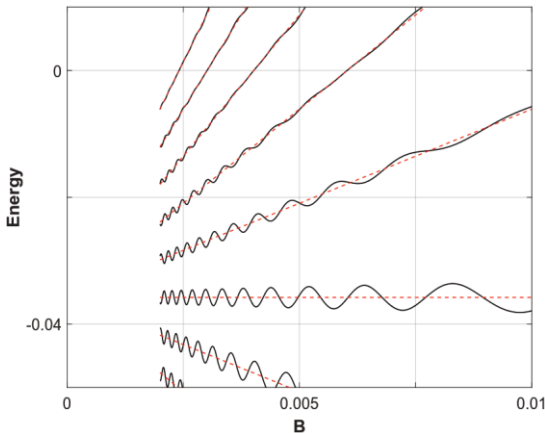
A single enlarged orbit

$$\Omega_1 + \Omega_2 = 2\pi(\mathbb{Z} + 1/2)$$

Incommensurate harmonics $(\Omega_1 \pm \Omega_2)/2 \rightarrow$ **quasirandom** spectrum

Level spacings are not equidistant, but exhibit long-range correlations.

Typical spectrum



$\mathcal{T} \approx 0$

Dominant harmonic $(\Omega_1 + \Omega_2)/2$ determines semiclassical Landau fan.

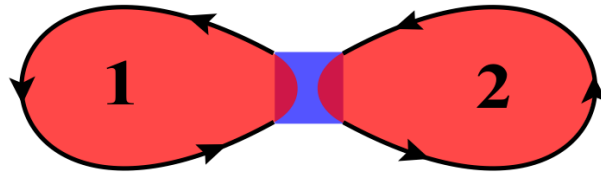
Leading-order tunneling correction oscillates with the frequency of $(\Omega_1 - \Omega_2)/2$.

We develop a perturbation theory for quasirandom spectra:

$$\delta E_j = \frac{\text{phase}(\mathcal{T}) + (-1)^j |\mathcal{T}| \cos\left(\frac{\Omega_1 - \Omega_2}{2}\right)}{-\frac{1}{2} \partial(\Omega_1 + \Omega_2) / \partial E}$$

Symmetry restores commensurability

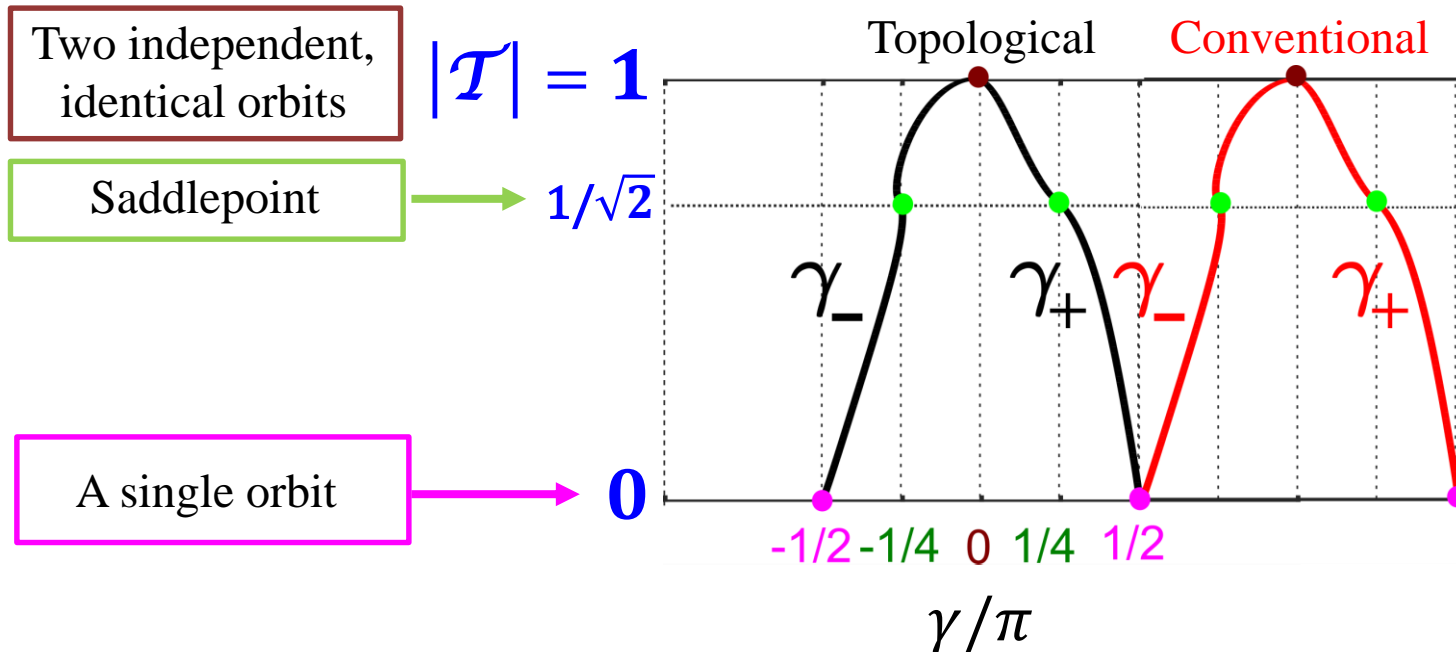
2D Dirac points are stabilized by spatial-inversion and time-reversal symmetry, e.g., graphene.

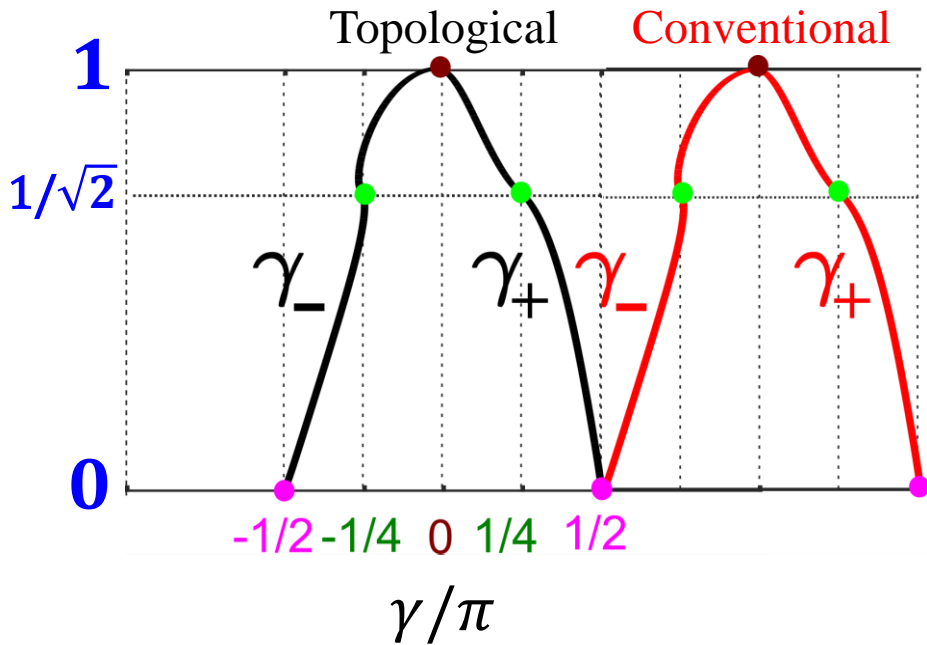


Saddlepoint is T-invariant

$$\cos\left(\frac{\Omega_1 + \Omega_2}{2} + \text{phase}(\mathcal{T})\right) = |\mathcal{T}|$$

Two dHvA harmonics with intercepts $\gamma_{\pm} = \varphi_B + \pi + \text{phase}(\mathcal{T}) - \cos^{-1}|\mathcal{T}|$





For both metals,
 $\gamma_{\pm}(\mu)$ covers a π -interval
 owing to the Lifshitz transition.

$$\gamma_{\pm} = \varphi_B + \pi + \underbrace{\text{phase}(\mathcal{T}) - \cos^{-1}|\mathcal{T}|}_{\text{topological invariant}}$$

A topological invariant that nonperturbatively encodes tunneling.

Analogy with topological insulators:
 as a function of crystal momentum,
 the Berry phase covers a 2π -interval

or a rational fraction of a 2π -interval

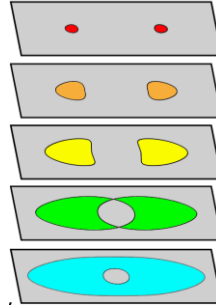
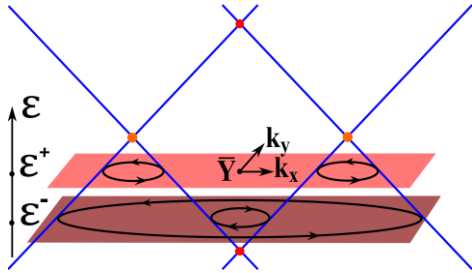
(Fu, Kane; Soluyanov, Vanderbilt; Rui Yu et al;
AA, X. Dai, Bernevig; AA, Z. Wang, Bernevig)

(AA, Bernevig, prb 93,205104; J. Hoeller, AA)

Unavoidable *intraband* breakdown in surface states of topological crystalline insulators.

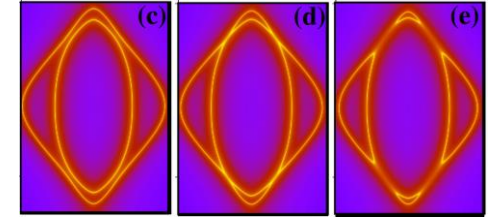
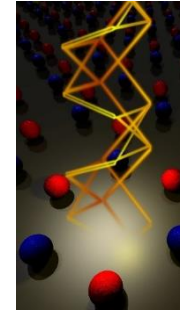
SnTe

(Hsieh, Liang Fu, Nat. Comm 3:982; Serbyn, Fu, PRB 90, 035402)



$$0 = \cos(\Omega_1 + 2\phi) + |\mathcal{R}|^2 \cos(\Omega_1 - \Omega_2) - |\mathcal{T}|^2$$

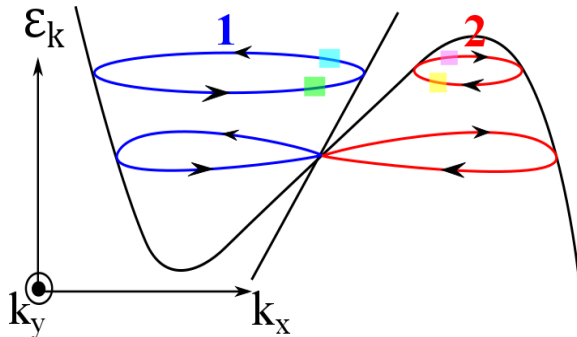
Hourglass fermion



(AA, Z. Wang, B.A. Bernevig, nature 532, 189; prx 6, 021008)

Unavoidable *interband* breakdown in over-tilted Dirac fermion

(O'Brien, Diez, Beenakker, PRL 116, 236401)

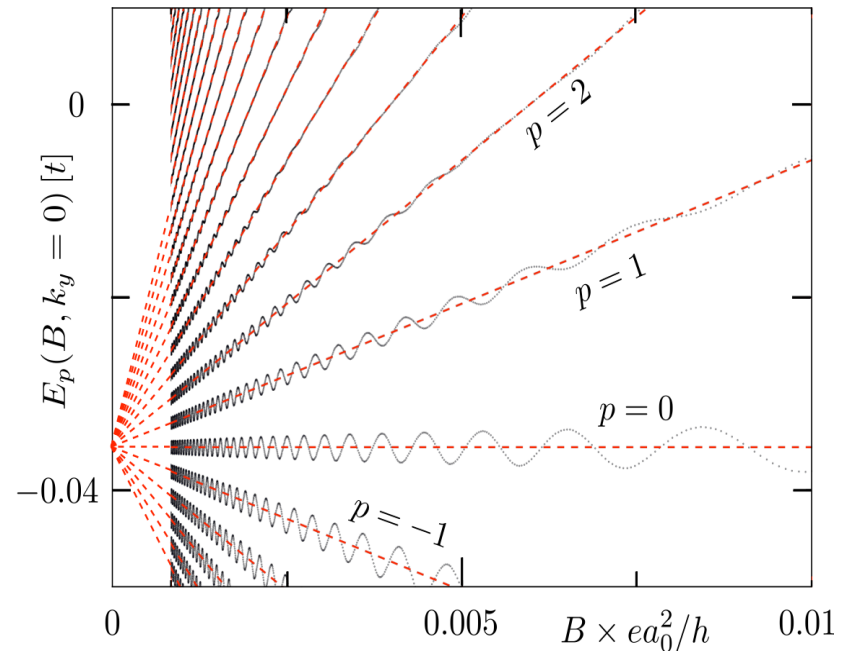
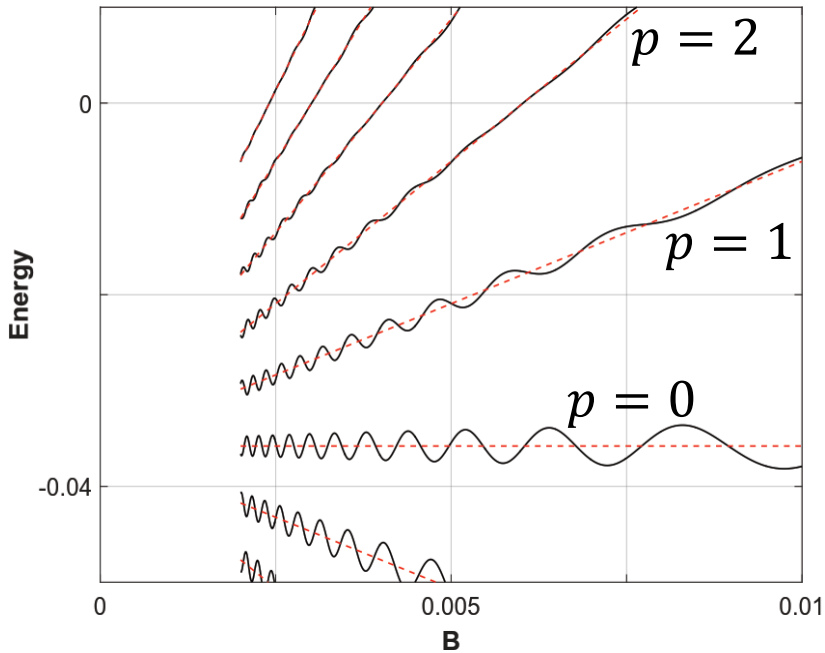
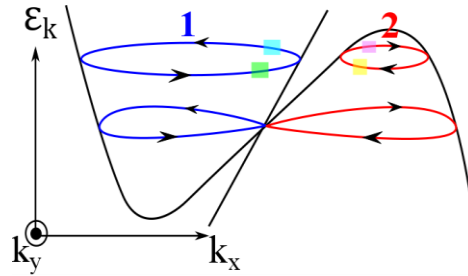


ρ^2 = Landau-Zener tunneling probability
= 1 at Dirac point

$$\cos\left(\frac{\Omega_1 - \Omega_2}{2}\right) = \sqrt{1 - \rho^2} \cos\left(\frac{\Omega_1 + \Omega_2}{2} + \omega\right)$$

Analytic method to calculate magnetic energy spectrum without large-scale numerical diagonalization

Test of generalized quantization rule with O'Brien tight-binding model of over-tilted Dirac fermion.
(Phys. Rev. Lett. 116, 236401)



Take-home

Fermiology: mapping the Fermi surface from the dHvA period.

Topo-fermiology: extracting robust information about Fermi-surface wavefunction from the dHvA intercept.

$$\gamma = \text{Maslov} + \text{Orbital moment} + \text{Berry} + \text{Zeeman}$$

For some solids, and for some field orientations, γ/π is rational.

Complete symmetry analysis of γ (10 classes of symmetric orbits)

In the presence of breakdown, generalized Bohr-Sommerfeld quantization conditions that encode the Berry phase and the orbital moment.

A modern theory of magnetic breakdown

When symmetry imposes commensurability,

$$\gamma = \text{Maslov} + \text{Berry} + \text{Tunneling phase}$$



A. Alexandradinata



Wang Chong



Leonid Glazman